

The cocrystal nicotineamide–succinic acid (2/1)

Laura J. Thompson, Raja S. Voguri, Adam Cowell, Louise Male and Maryjane Tremayne*

School of Chemistry, University of Birmingham, Edgbaston, Birmingham B15 2TT, England

Correspondence e-mail: m.tremayne@bham.ac.uk

Received 1 July 2010

Accepted 9 July 2010

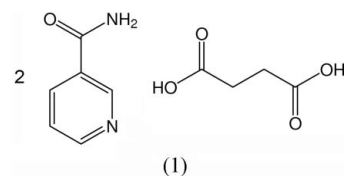
Online 20 July 2010

In the asymmetric unit of the crystal structure of nicotineamide–succinic acid (2/1), $2C_6H_6N_2O \cdot C_4H_6O_4$, there are two independent nicotineamide molecules in general positions and two half succinic acid molecules which lie about inversion centres. The structure contains acid–pyridine and amide–amide synthons with nicotineamide molecules forming ladders of alternating $R_2^2(8)$ and $R_4^2(8)$ rings linked through succinic acid to generate a corrugated hydrogen-bonded sheet. This sheet is a common supramolecular unit found in other 2:1 nicotineamide–dicarboxylic acid cocrystals, but the presence of two crystallographically distinct nicotineamides with *anti* and *syn* conformations, forming two distinct sheets within the same structure, is a novel packing feature in this type of material.

Comment

Molecular cocrystals are becoming increasingly important within the pharmaceutical industry as they represent a new source of solid-state materials which have the potential to provide optimal physical properties while retaining the chemical properties of the individual components (Almarsson & Zaworotko, 2004; Vishweshwar *et al.*, 2006; Blagden *et al.*, 2008). However, successful synthesis of these multicomponent materials relies on the preferential formation of heteromeric synthons rather than the formation of strong interactions within the structures of the individual cocrystal formers. Both nicotineamide and isonicotinic acid have demonstrated the propensity for cocrystal formation with a range of carboxylic acids (Aakeröy *et al.*, 2002; Vishweshwar *et al.*, 2003; Chakrabarty *et al.*, 2006; Amai *et al.*, 2006; Schmidtman *et al.*, 2007; Karki *et al.*, 2009; Orola *et al.*, 2009), showing consistent preference for the formation of a heteromeric acid–pyridine hydrogen bond, (I) (Fig. 1). The formation of an amide–amide, (II), or acid–amide, (III), hydrogen bond (Fig. 1) is then dependent on the stoichiometry of the cocrystal; those formed with a monocarboxylic acid in a 1:1 ratio or with a dicarboxylic acid in a 2:1 ratio show a preference for the formation of

synthon (II), whereas cocrystals with the dicarboxylic acid in a 1:1 ratio tend to form synthon (III). This is clearly illustrated in cases where both 1:1 and 2:1 cocrystal stoichiometries have been identified; for example, nicotineamide–adipic acid, nicotineamide–suberic acid (Karki *et al.*, 2009), nicotineamide–fumaric acid (Orola *et al.*, 2009), isonicotinic acid–glutaric acid and isonicotinic acid–adipic acid (Vishweshwar *et al.*, 2003).



We report here the crystal structure of the nicotineamide–succinic acid 2:1 cocrystal, (1). Cocrystal (1) was prepared by slow evaporation from a 1:1 stoichiometric ratio of starting materials as described previously, although no crystal structure was reported in that case (Karki *et al.*, 2009).

The crystal structure of (1) displays an extended hydrogen-bond network generated by the acid–pyridine and amide–amide synthons expected in a cocrystal of this composition in a 2:1 stoichiometry, but unlike other nicotineamide–acid cocrystals, (1) contains two crystallographically distinct nicotineamide molecules with different conformations. Nicotineamide molecule *A* (denoted by atom labels ‘a’ in Fig. 2) adopts an *anti* conformation with the heterocyclic N and amide N on opposite sides of the molecule [torsion angle $C6A-C5A-C7A-N7A = 151.9(2)^\circ$; Table 1] whereas nicotineamide molecule *B* (denoted by atom labels ‘b’ in Fig. 2) adopts a *syn* conformation [torsion angle $C6B-C5B-C7B-N7B = 26.5(3)^\circ$; Table 1]. A search of the Cambridge Structural Database (Allen, 2002) revealed that in other nicotineamide adducts the nicotineamide molecule displays only one conformation in each structure (either the *anti* or *syn*), and there are more examples of structures adopting the *anti* rather than the *syn* conformation. An electron-density map was used to identify the posi-

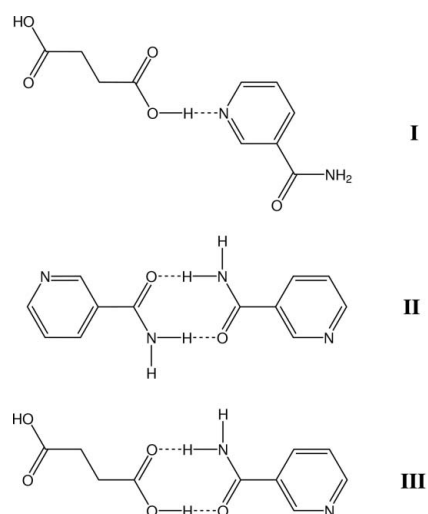
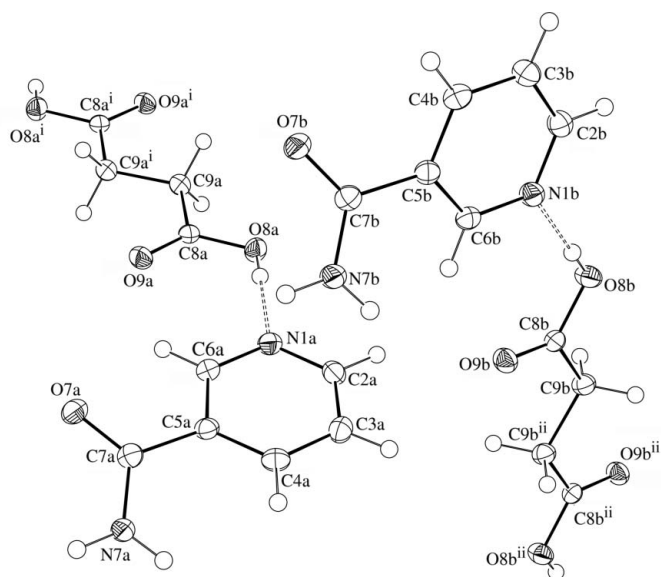
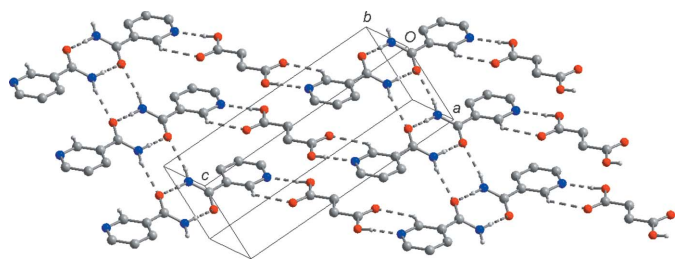


Figure 1
Potential hydrogen-bond synthons found in acid–amide cocrystals.

**Figure 2**

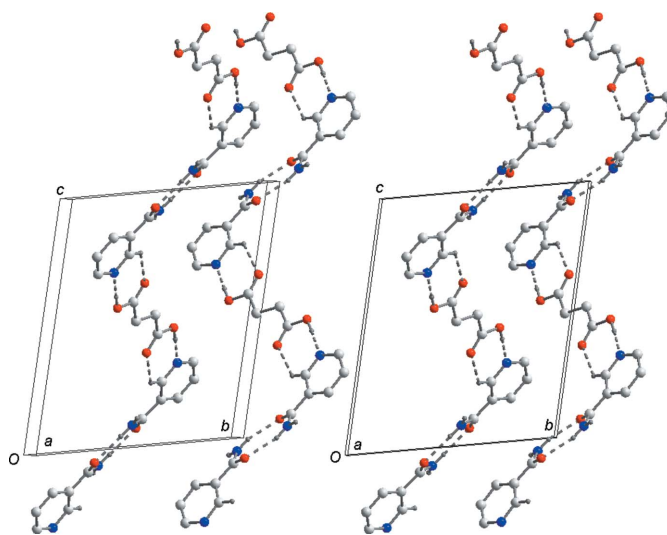
The independent molecules of (1), showing the atom-numbering scheme and the hard intermolecular hydrogen bonds (dashed lines). Displacement ellipsoids are drawn at the 50% probability level and H atoms are shown as small spheres of arbitrary radii. [Symmetry codes: (i) $-x + 3, -y + 2, -z + 1$; (ii) $-x, -y + 1, -z + 1$.]

**Figure 3**

A view of the corrugated hydrogen-bonded sheet in the ac plane formed by nicotinamide *A* and succinic acid *A* molecules. Hydrogen bonds are shown as dashed lines. H atoms not involved in hydrogen bonding have been omitted for clarity.

tions of the carboxyl H atoms (H8A and H8B) in (1), confirming that this is a neutral cocrystal form rather than a salt (see *Experimental*).

Each nicotinamide molecule (*A* and *B*) is involved in four intermolecular hydrogen bonds with *A* and *B* molecules, respectively; one hard O—H...N(heterocyclic) interaction and one soft C—H...O=C hydrogen bond to a succinic acid molecule, and two hard N—H...O=C hydrogen bonds to other nicotinamide molecules of the same conformation (Table 2). More specifically, the carboxyl oxygen O8A acts as a hydrogen-bond donor, *via* H8A, to heterocyclic atom N1A of nicotinamide *A* at (x, y, z) with the acid–pyridine packing motif (I) reinforced by C6A in the nicotinamide acting as a soft hydrogen-bond donor through H6A to the other carboxyl oxygen O9A at (x, y, z) . Propagation of this motif through inversion within the succinic acid molecule generates the 2:1 nicotinamide–succinic acid unit in which succinic acid *A* is capped at both ends by molecules of nicotinamide *A*. These units are then linked together through a complementary

**Figure 4**

A stereoview of part of the crystal structure of (1), showing the chains formed by nicotinamide *A* and succinic acid *A* molecules running along $[20\bar{1}]$ (right) and by nicotinamide *B* and succinic acid *B* molecules running along $[201]$ (left). Hydrogen bonds are shown as dashed lines. H atoms not involved in hydrogen bonding have been omitted for clarity.

amide dimer $R_2^2(8)$ motif, (II) (Bernstein *et al.*, 1995), formed by N7A *via* H7AA to O7A at $(1 - x, 2 - y, 2 - z)$ to generate a chain running in the $[20\bar{1}]$ direction. The chains are linked through a second complementary N—H...O interaction formed by N7A through H7AB donation to O7A at $(-1 + x, y, z)$, resulting in the formation of ladders of alternating $R_4^2(8)$ and $R_2^2(8)$ rings and the generation of an extended corrugated hydrogen-bonded sheet in the ac plane (Fig. 3).

Nicotinamide *B* is involved in a similar set of intermolecular interactions with succinic acid *B* and other nicotinamide *B* molecules, generating the same synthons and motifs as nicotinamide *A*. The formation of a dimer with nicotinamide *B* at $(2 - x, 1 - y, 2 - z)$ generates a chain linking the 2:1 nicotinamide *B*–succinic acid *B* units, which in this case runs in the $[201]$ direction. These chains are then linked to others to give a second corrugated hydrogen-bonded sheet also in the ac plane. Hence, the structure of (1) contains alternating sheets comprised purely of *A* molecules and then purely of *B* molecules in which the chains run in opposing directions (Fig. 4). There are no strong interactions between alternating sheets and all strong hydrogen-bond donors and acceptors are used in the hydrogen-bond network.

The corrugated hydrogen-bonded sheet formed by nicotinamide *A* in the *anti* conformation is a common supramolecular unit found in other 2:1 nicotinamide–dicarboxylic acid cocrystals in which the alkyl chain in the acid is longer, such as nicotinamide–adipic acid, nicotinamide–suberic acid and nicotinamide–sebacic acid (Karki *et al.*, 2009). Similar *anti* conformation chains are also formed by 2:1 cocrystals with malonic and fumaric acids, but in these cases the chains are linked through a further acid–amide interaction rather than through the formation of nicotinamide ladders. There are no other reports of the *syn* conformation in this series of cocrystals, although it is found in the synthon (III)-based acid–

amide chains formed in the 1:1 stoichiometry nicotinamide: glutaric acid and nicotinamide–pimelic acid cocrystals (Karki *et al.*, 2009).

In conclusion, the single-crystal structure of (1) highlights the formation of a supramolecular hydrogen-bonded sheet that is also seen in other nicotinamide–dicarboxylic acid cocrystals of this stoichiometry. However, the formation of two distinct sheets with *anti* and *syn* nicotinamide conformations is a novel packing feature in this type of material. This display of both typical and atypical structural behaviour within (1) may be (i) a result of the succinic acid being at the interface of two distinct preferred packing modes dependent on the size of the acid component, or (ii) an indication that other packing modes may be exhibited through potential polymorphic behaviour.

Experimental

All starting materials were purchased from Sigma Aldrich and used without purification. Nicotinamide (0.0138 g, 1.13×10^{-4} mmol) and succinic acid (0.0133 g, 1.13×10^{-4} mmol) were dissolved in warm methanol (5 ml) in a 1:1 stoichiometric ratio. The resulting solution was cooled to room temperature and, on slow evaporation of the solvent, crystals were formed. A colourless lath-shaped crystal of (1) was selected and used for single-crystal X-ray diffraction.

Crystal data

$2C_6H_6N_2O \cdot C_4H_6O_4$	$\gamma = 89.418 (2)^\circ$
$M_r = 362.34$	$V = 818.01 (6) \text{ \AA}^3$
Triclinic, $P\bar{1}$	$Z = 2$
$a = 5.0872 (2) \text{ \AA}$	Mo $K\alpha$ radiation
$b = 11.5569 (5) \text{ \AA}$	$\mu = 0.12 \text{ mm}^{-1}$
$c = 14.2784 (5) \text{ \AA}$	$T = 120 \text{ K}$
$\alpha = 77.433 (2)^\circ$	$0.17 \times 0.03 \times 0.01 \text{ mm}$
$\beta = 86.726 (2)^\circ$	

Data collection

Bruker–Nonius APEXII CCD camera on κ -goniostat diffractometer	12664 measured reflections
Absorption correction: multi-scan (SADABS; Sheldrick, 2007)	3205 independent reflections
$T_{\min} = 0.981$, $T_{\max} = 0.999$	2455 reflections with $I > 2\sigma(I)$
	$R_{\text{int}} = 0.061$

Refinement

$R[F^2 > 2\sigma(F^2)] = 0.056$	237 parameters
$wR(F^2) = 0.132$	H-atom parameters constrained
$S = 1.11$	$\Delta\rho_{\text{max}} = 0.24 \text{ e \AA}^{-3}$
3205 reflections	$\Delta\rho_{\text{min}} = -0.27 \text{ e \AA}^{-3}$

The presence of atoms H8A and H8B bonded to O8A and O8B, respectively [showing (1) is a cocrystal rather than a salt], was confirmed by the observation of peaks in those locations in an electron-density map, in addition to analysis of the C8A/B–O8A/B and C8A/B–O9A/B bond lengths (Table 1). All H atoms were then added at calculated positions and refined using a riding model, with C–H = 0.95 Å for aromatic H atoms, 0.99 Å for methylene H atoms, N–H = 0.88 Å and O–H = 0.84 Å and with $U_{\text{iso}}(\text{H}) = 1.2U_{\text{eq}}(\text{C})$, $1.2U_{\text{eq}}(\text{N})$ and $1.5U_{\text{eq}}(\text{O})$. In the case of the O8A–H8A and O8B–H8B groups, the riding model used (AFIX 147) allowed the chosen C–C–O–H torsion angle to maximize the electron density at the calculated H-atom position such that the final positions for H8A and

Table 1

Selected geometric parameters (Å, °).

C7A–O7A	1.241 (3)	C7B–O7B	1.242 (3)
C7A–N7A	1.332 (3)	C7B–N7B	1.331 (3)
C8A–O9A	1.213 (3)	C8B–O9B	1.212 (3)
C8A–O8A	1.328 (3)	C8B–O8B	1.334 (3)
O7A–C7A–N7A	121.8 (2)	O7B–C7B–N7B	122.2 (2)
O9A–C8A–O8A	123.6 (2)	O9B–C8B–O8B	123.3 (2)
C6A–C5A–C7A–N7A	151.9 (2)	C6B–C5B–C7B–N7B	26.5 (3)
O8A–C8A–C9A–C9A ⁱ	176.4 (2)	O8B–C8B–C9B–C9B ⁱⁱ	–176.6 (2)

Symmetry codes: (i) $-x + 3, -y + 2, -z + 1$; (ii) $-x, -y + 1, -z + 1$.

Table 2

Intermolecular hydrogen-bonding and weak interactions (Å, °) for (1).

$D-H \cdots A$	$D-H$	$H \cdots A$	$D \cdots A$	$D-H \cdots A$
O8A–H8A \cdots N1A	0.84	1.85	2.691 (3)	174.1
C6A–H6A \cdots O9A	0.95	2.52	3.206 (3)	129.5
N7A–H7AA \cdots O7A ⁱⁱⁱ	0.88	2.10	2.953 (3)	164.1
N7A–H7AB \cdots O7A ^{iv}	0.88	2.15	2.899 (3)	142.2
O8B–H8B \cdots N1B	0.84	1.84	2.682 (3)	176.0
C6B–H6B \cdots O9B	0.95	2.61	3.268 (3)	126.9
N7B–H7BA \cdots O7B ^v	0.88	2.06	2.941 (3)	173.6
N7B–H7BB \cdots O7B ^{iv}	0.88	2.22	2.947 (3)	139.1

Symmetry codes: (iii) $-x + 1, -y + 2, -z + 2$; (iv) $x - 1, y, z$; (v) $-x + 2, -y + 1, -z + 2$.

H8B are very close to the peaks initially observed in the electron-density map.

Data collection: COLLECT (Hooft, 1998); cell refinement: DENZO (Otwinowski & Minor, 1997) and COLLECT; data reduction: DENZO and COLLECT; program(s) used to solve structure: SHELXS97 (Sheldrick, 2008); program(s) used to refine structure: SHELXL97 (Sheldrick, 2008); molecular graphics: ORTEP-3 for Windows (Farrugia, 1997) and DIAMOND (Brandenburg & Putz, 1999); software used to prepare material for publication: WinGX (Farrugia, 1999).

We thank the University of Birmingham and the EPSRC for the support for LJT, RSV and AC. The EPSRC National Crystallography Service is thanked for collection of the single-crystal X-ray diffraction data. The powder diffraction facilities used in this research were obtained through the Science City Advanced Materials project with support from Advantage West Midlands (AWM) and part funded by the European Regional Development Fund (ERDF).

Supplementary data for this paper are available from the IUCr electronic archives (Reference: FG3180). Services for accessing these data are described at the back of the journal.

References

- Aakeröy, C. B., Beatty, A. M. & Helfrich, B. A. (2002). *J. Am. Chem. Soc.* **124**, 14425–14432.
- Allen, F. H. (2002). *Acta Cryst.* **B58**, 380–388.
- Almarsson, O. & Zaworotko, M. J. (2004). *Chem. Commun.* pp. 1889–1896.
- Amari, M., Kamijo, M., Nagase, H., Ogawa, N., Endo, T. & Ueda, H. (2006). *Anal. Sci.* **22**, x121–x122.
- Bernstein, J., Davis, R. E., Shimoni, L. & Chang, N. L. (1995). *Angew. Chem. Int. Ed. Engl.* **34**, 1555–1573.

- Blagden, N., Berry, D. J., Parkin, A., Javed, H., Ibrahim, A., Gavan, P. T., De Matos, L. L. & Seaton, C. C. (2008). *New J. Chem.* **32**, 1659–1672.
- Brandenburg, K. & Putz, H. (1999). *DIAMOND*. Crystal Impact GbR, Bonn, Germany.
- Chakrabarty, D., Nagase, H., Kamijo, M., Endo, T. & Ueda, H. (2006). *Anal. Sci.* **22**, x27–x28.
- Farrugia, L. J. (1997). *J. Appl. Cryst.* **30**, 565.
- Farrugia, L. J. (1999). *J. Appl. Cryst.* **32**, 837–838.
- Hooft, R. W. W. (1998). *COLLECT*. Nonius BV, Delft, The Netherlands.
- Karki, S., Friscic, T. & Jones, W. (2009). *CrystEngComm*, **11**, 470–481.
- Orola, L. & Veidis, M. V. (2009). *CrystEngComm*, **11**, 415–417.
- Otwinowski, Z. & Minor, W. (1997). *Methods in Enzymology*, Vol. 276, *Macromolecular Crystallography*, Part A, edited by C. W. Carter Jr & R. M. Sweet, pp. 307–326. New York: Academic Press.
- Schmidtman, M., Gutmann, M. J., Middlemiss, D. S. & Wilson, C. C. (2007). *CrystEngComm*, **9**, 743–745.
- Sheldrick, G. M. (2007). *SADABS*. University of Göttingen, Germany.
- Sheldrick, G. M. (2008). *Acta Cryst.* **A64**, 112–122.
- Vishweshwar, P., McMahon, J. A., Bis, J. A. & Zaworotko, M. J. (2006). *J. Pharm. Sci.* **95**, 499–516.
- Vishweshwar, P., Nangia, A. & Lynch, V. M. (2003). *Cryst. Growth Des.* **3**, 783–790.